SERMeQ model produces a realistic upper bound on calving retreat for 155 Greenland outlet glaciers

Lizz Ultee[1], Jeremy N. Bassis[2]

[1]Department of Earth, Atmospheric, and Planetary Sciences, Massachusetts Institute of Technology, Cambridge, MA, 02139

[2]Department of Climate & Space Sciences, University of Michigan, Ann Arbor, MI 48109

Key Points:

- We tested an upper-bound model of calving retreat of 155 ocean-terminating outlet glaciers that drain the Greenland Ice Sheet.
- Our physics-based method produces terminus positions that correlate with observed positions for 103 glaciers without model tuning.
- Our model bounds retreat rates on 91% of glaciers tested, providing a constraint for future sea level projections.

Corresponding author: Lizz Ultee, `ehultee@umich.edu`

Abstract

The rate of land ice loss due to iceberg calving is a key source of variability among model projections of 21st century sea-level rise. It is especially challenging to account for mass loss due to iceberg calving in Greenland, where ice drains to the ocean through hundreds of outlet glaciers, many smaller than typical model grid scale. Here, we apply a numerically efficient network flowline model (SERMeQ) forced by surface mass balance to simulate an upper bound on decadal calving retreat of 155 grounded outlet glaciers of the Greenland Ice Sheet—resolving five times as many outlets as was previously possible. We show that the upper bound holds for 91% of glaciers examined and that simulated changes in terminus position correlate with observed changes. SERMeQ can provide a physically consistent constraint on forward projections of the dynamic mass loss from the Greenland Ice Sheet associated with different climate projections.

1 Introduction

The Greenland Ice Sheet is currently the largest single contributor to global mean sea level rise (van den Broeke et al., 2017). It discharges ice mass to the ocean through three main processes: release of surface meltwater, submarine melting where ice is in contact with the ocean, and the detachment (calving) of icebergs. The ice mass lost to submarine melting has only recently been directly observed (Sutherland et al., 2019) and remains difficult to estimate for the whole ice sheet (Beckmann et al., 2018), but it is clear that enhanced surface melting and calving processes have resulted in increased mass discharge since the late 1990s (van den Broeke et al., 2016; Enderlin et al., 2014; Khan et al., 2014).

Processes that control surface melt are increasingly resolved in regional models (Mottram et al., 2017; Noël et al., 2018). Iceberg calving, by contrast, remains poorly understood, with multiple contradictory parameterizations incorporated into ice sheet/glacier models (Benn, Cowton, et al., 2017; Morlighem et al., 2016; Levermann et al., 2012). Furthermore, iceberg calving can remove mass more rapidly than is possible through melting alone, contributing to rapid tidewater glacier retreat through mechanisms like tidewater glacier instability (Meier & Post, 1987) and the recently-described Marine Ice Cliff Instability (Bassis & Walker, 2012; Pollard et al., 2015).

Simulating discharge from the Greenland Ice Sheet is further complicated by the local factors affecting ice discharge at the nearly 200 outlet glaciers that connect the ice sheet to the ocean (e.g. Catania et al., 2018; Enderlin et al., 2018). For all but the largest outlets, iceberg calving occurs at smaller scales than are captured in continental-scale ice sheet models. Existing estimates of dynamic mass loss from Greenland outlets have come from extrapolating perturbations on the largest outlets (Price et al., 2011; Nick et al., 2013), simulating the sea level contribution from only selected outlets (Choi et al., 2017; Morlighem et al., 2019), or simulating the entire ice sheet at a spatial resolution of 500 m (Aschwanden et al., 2016, 2019) to resolve about 30 of the nearly 200 glaciers that drain the Greenland Ice Sheet.

Despite these achievements, more than 100 outlet glaciers, responsible for $\sim 1/3$ of current Greenland Ice Sheet discharge (Enderlin et al., 2014), are not routinely simulated, and their dynamics cannot necessarily be inferred from the dynamics of larger outlets. Another layer of spatial complexity arises in that many outlet glaciers collect ice from several interacting tributary branches that are themselves also smaller than typical ice sheet model grid scale. The small scale of tributary glacier networks feeding outlets makes them especially challenging to simulate in continental ice sheet models, requiring model resolution of hundreds to tens of meters to adequately resolve.

A more fundamental challenge in projecting mass loss due to calving is the incompatibility of fracture-driven iceberg calving with the assumption of continuum deforma-

tion inherent in most ice sheet models (e.g. Price et al., 2015; Winkelmann et al., 2011; Greve, 2000). Simple empirical parameterizations can relate calving rate to continuous variables, such as proglacial water depth (Brown et al., 1982; Hanson & Hooke, 2000), but may not hold into the future as climate forcing enters a new statistical regime. Physically-based calving laws, such as the fracture field approach developed by Albrecht and Levermann (2012) or von Mises calving law developed for Greenland by Morlighem et al. (2016), often impose an empirically-adjustable calving rate parameter. Recent work has sought to simulate ice failure using continuum damage mechanics, with some success in a variety of case studies (Borstad et al., 2012; Duddu et al., 2013; Krug et al., 2014; Sun et al., 2017; Mercenier et al., 2019). However, at present the evolution of the damage field through a damage production function is also empirical, with multiple tuned parameters that are poorly constrained by laboratory or field measurements (Emetc et al., 2018). Another recent approach couples a granular model that allows true fracture and calving to a finite-element model that solves an approximation to the Stokes equations for viscous deformation, offering a very promising basis for process-scale simulation of fully-dynamic calving (Benn, Åström, et al., 2017). Unfortunately, the coupled approach remains too computationally expensive for century-scale projections. Despite their promise, neither continuum damage models nor granular calving models have been able to reproduce observed multi-annual evolution of calving front positions in Greenland.

Improving projections of 21st-century sea level rise requires models that can *(i)* reproduce complex patterns of glacier advance and retreat currently observed in Greenland and *(ii)* efficiently simulate dynamic discharge and iceberg calving from individual outlet glaciers for a spectrum of climate scenarios. To address this, we have developed a simple model to simulate advance, retreat, and dynamic mass loss due to calving on networks of marine-terminating glaciers (Ultee & Bassis, 2016, 2017; Bassis & Ultee, 2019). Our model framework, called SERMeQ, is able to directly simulate decade-to-century-scale evolution of hundreds of outlet glaciers in response to surface mass balance forcing across multiple climate scenarios. This explicit simulation capability, together with recent observations of more than 200 Greenland outlet glacier termini (Joughin et al., 2015, updated 2017a), makes it possible to evaluate our model's performance in a wide range of glacier environments. Here, we show that SERMeQ bounds retreat rates, and reproduces patterns of present-day observed changes in terminus position of 155 Greenland outlet glaciers, providing one of the largest validations of any calving parameterization. On the basis of this validation, our model physics can be incorporated into global glacier and ice sheet models to compute a physically-consistent upper constraint on the century-scale glaciological contribution to global sea level rise.

2 Methods

2.1 SERMeQ ice dynamics model

SERMeQ—the Simple Estimator of Retreat Magnitude and ice flux (Q), *sermeq* meaning "glacier" in Greenlandic—is a width-averaged, vertically-integrated model that determines centerline glacier surface elevation corresponding to a given terminus position. The ice dynamics are based on a perfectly-plastic limiting case of a viscoplastic rheology (Nye, 1951; Bassis & Ultee, 2019), with modifications to allow calving at a grounded ice-water interface (Ultee & Bassis, 2016) and interaction between multiple tributary glaciers (Ultee & Bassis, 2017). Our flowline-modeling approach is compatible with other flowline-based models such as the Open Global Glacier Model (Maussion et al., 2019), but SERMeQ focuses specifically on near-terminus dynamics of marine glaciers to simulate the calving process.

Rather than imposing an empirical calving rate, SERMeQ self-consistently calculates the maximum rate of terminus advance or retreat at each time step for a given climate forcing. Terminus position evolves in response to near-terminus stretching, bedrock

topography, and changes in catchment-wide surface mass balance as described in Ultee (2018) and Bassis and Ultee (2019),

$$\frac{dL}{dt} = \frac{\dot{a} - H\frac{\partial U}{\partial x} - U\frac{\partial H}{\partial x}}{\frac{\partial H_y}{\partial x} - \frac{\partial H}{\partial x}} \ . \tag{1}$$

In Equation 1, $H = H(x,t)$ is the ice thickness, $U = U(x,t)$ the ice velocity, $\dot{a} = \dot{a}(x,t)$ the net ice accumulation rate, H_y the thickness at which effective stress within the ice reaches its yield strength (Equation S1), and all terms are evaluated at the instantaneous terminus position, $x = L(t)$ (see Supplementary Text S1-2). For a change in terminus position determined from Equation 1, SERMeQ calculates a new steady-state glacier surface elevation profile and calculates change in glacier volume above buoyancy (Supplementary Figure S1). The latter produces a net contribution to global mean sea level (example in Supplementary Text S1, not evaluated in this validation exercise).

The only adjustable model parameters are ice temperature T, which is used to calculate the horizontal stretching rate $\partial U/\partial x$ at the terminus, and yield strength τ_y, which is used to calculate the yield thickness H_y (Supplementary Text S1-S3). Both are material quantities that can be independently constrained by laboratory and field measurements. Crucially, we do not tune either of our parameters to match changes in terminus position. Comparison of simulated with observed terminus position thus provides a completely independent validation.

Here, we extend the physical realism and applicability of our model to demonstrate that it can simulate calving retreat of a wide variety of marine-terminating glaciers. Novel elements of SERMeQ specific to this application include upstream forcing with surface mass balance from a regional climate model (Mottram et al., 2018) and the automatic selection of networks of flowlines with varying width (traced from Joughin et al., 2015, updated 2017b, see Supplementary Text S5).

2.2 Identification of flowline networks

We first identified 181 Greenland outlet glaciers that have multiple terminus positions recorded in Joughin et al. (2015, updated 2017a). For each glacier, we then defined a network of interacting flowlines with spatially variable width by tracing ice surface velocity from Joughin et al. (2015, updated 2017b, and see Supplementary Text S5). We extracted ice surface and bed elevation from BedMachine version 3 (Morlighem et al., 2017) and applied a Gaussian filter to produce width-averaged topography. Where the data suggested the presence of short, transient ice tongues, we removed the floating portion from consideration and simulated the grounding line as the "terminus". We removed three glaciers with long, persistent ice tongues, as SERMeQ is unable to simulate ice tongue evolution. Thirteen of the 181 outlets had initial termini grounded above sea level and iceberg calving is thus unlikely to dominate dynamic mass changes there. We removed those thirteen glaciers from consideration as well. Noisy or missing data that produced unphysical bed topography caused us to remove ten additional outlets, leaving 155 glaciers for our analysis.

For the remaining 155 outlet glaciers, we defined the initial terminus as the grounded-ice point along our central flowline that lies closest to the centroid of the 2006 terminus reported in Joughin et al. (2015, updated 2017a). We optimized a single parameter, the yield strength of ice, to best fit the 2006 observed surface profile, as described in Ultee and Bassis (2017). We used a best-guess ice temperature T of $-10°$ C for all glaciers. We then found the catchment-wide, annual mean surface mass balance forcing for each outlet, $\dot{a}$ in Equation 1, from HIRHAM regional climate model reanalysis (Mottram et al., 2018; Rae et al., 2012; Lucas-Picher et al., 2012), and simulated resulting changes between 2006 and 2014 in ice extent (Figures 1-3) and volume above buoyancy (Figure 4 and Supplementary Figure 1). Finally, we compared the simulated changes in termi-

nus position with observed changes reported in Joughin et al. (2015, updated 2017a) for the same period. Because our optimization of τ_y considers only the initial observed surface profile, and the changes in terminus position are an independent response to changes in surface mass balance, this comparison examines an independent model prediction that is not tuned to match observations.

2.3 Comparison with observations

We extracted all available terminus position records from (Joughin et al., 2015, updated 2017a) for each year within our simulated period: 2006, 2007, 2009, 2013, and 2014. Each terminus position record consists of one or more points; records with multiple points trace across-flow variation in terminus position. We projected all available points from a given record onto the central flowline of the corresponding glacier network, and we identified the space between the most seaward and most landward points of that projection as the "observational range". We also tracked the change over time in the position of the terminus centroid projected on the flowline, which we identified as the "observed (terminus-centroid) retreat rate". Finally, we compared the simulated retreat rates with the observed terminus-centroid retreat rates (Figure 2) and the simulated terminus positions with the observational range (Figures 3-4a).

3 Results

3.1 An upper bound on calving retreat for 155 Greenland outlets

Figure 1 shows the total retreat we simulated for each glacier between 2006 and 2014, arranged by approximate outlet position. SERMeQ simulates less than 5 km of length change during the observed period on most outlets. There is no relationship between outlet glacier latitude and magnitude of upper-bound retreat: simulated glacier response to downscaled climate reanalysis forcing is not a simple function of annual average temperature. Dynamic glacier response depends on glacier geometry, as previous studies have also highlighted (Felikson et al., 2017; Benn, Cowton, et al., 2017; Catania et al., 2018).

Equation 1 includes an assumption that the glacier calving front is a yield surface, which produces a theoretical upper bound on calving retreat for a given glacier geometry and surface mass balance (see Bassis & Ultee, 2019). Thus, provided there are no significant errors in the bed geometry and surface mass balance used, we anticipate that SERMeQ-simulated rates of retreat will generally overestimate observed rates. Figure 2 shows that SERMeQ satisfies this expectation and overestimates retreat for 91% (108/119) of glaciers for which more than two terminus position observations are available to constrain the observed retreat rate.

The bulk model results shown in Figures 1 and 2 summarize multi-annual change in terminus position simulated across Greenland. Figure 3 compares observed and simulated terminus position change for example glaciers where SERMeQ underestimates, overestimates, or correctly captures the observed rate of retreat. Apuseeq Anittangasikkaa-juk, which is 2 km wide at the terminus and has a small floating ice tongue, is one of a handful of outlets where SERMeQ underestimates observed retreat (Fig. 3a). The simulated terminus positions are still within the (small) observational range in that case. SERMeQ strongly overestimates retreat of Helheim Glacier, a large and high-flux glacier on Greenland's east coast whose terminus approaches flotation (Fig. 3b). On Sermeq Kujalleq (Danish: Jakobshavn Isbræ), a very large and well-studied outlet glacier on the southwest coast of Greenland, the simulated retreat of 6 km is comparable to observed retreat (Fig. 3c).
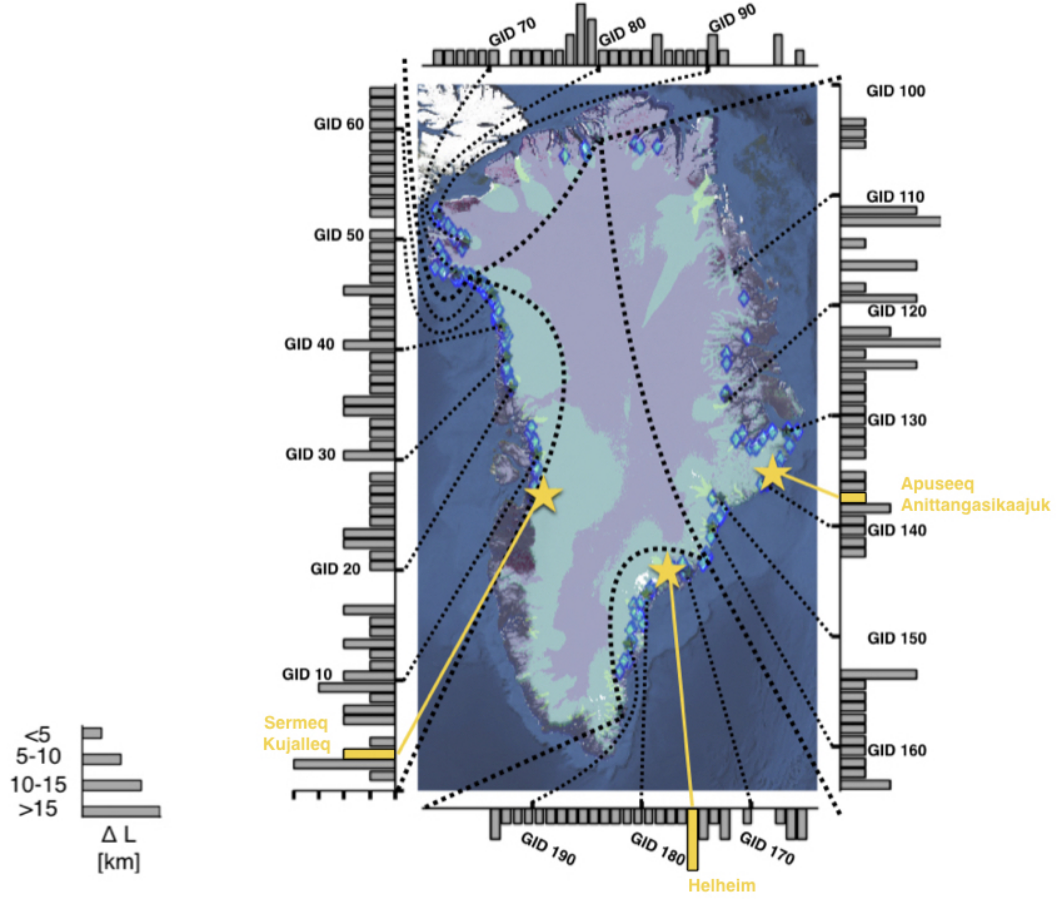
Figure 1. Map view of the 2006-2014 retreat simulated in this work. Bars indicate magnitude of simulated retreat for each glacier, with glaciers identified and ordered by their MEaSUREs outlet glacier ID number (1-200). Glacier ID 1, which is in the Disko Bay region, appears in the lower left; glacier IDs increase clockwise around the map border. Blue diamonds mark the map location of each outlet we simulated, and every 10th glacier ID is labelled and connected to its outlet location in black. A table of MEaSUREs glacier IDs and names appears in the Supplementary Material. Border spaces with no bar correspond to outlets where data was not sufficient to initialize a SERMeQ simulation, or where our analysis indicated SERMeQ would not be applicable (see Section 2). Yellow bars and map stars show the case-study glaciers highlighted in Figure 3. Coloured overlay on the satellite map is ice velocity derived from Sentinel-1 observations (ENVEO, 2017), shown on a logarithmic scale such that fast-moving outlet networks appear brighter than slow-moving inland ice.
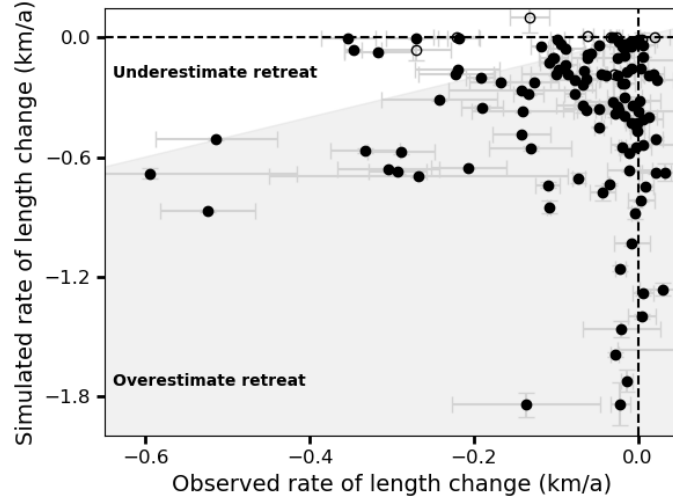
Figure 2. Comparison of observed and simulated rate of retreat for all glaciers simulated. Markers indicate the slope of linear fits to the observed (x-axis) and simulated (y-axis) terminus positions over the 2006-2014 period. Error bars indicate the error on each linear regression. Open circles indicate oscillating termini that are not well captured by linear regression to simulated position (p>0.05; $n = 9$).
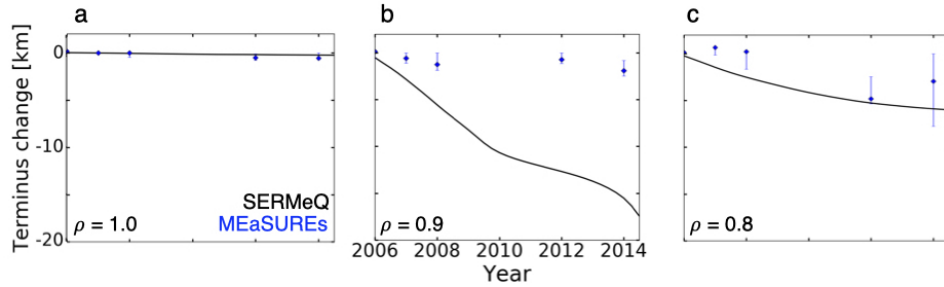

Figure 3. Comparisons of observed and simulated terminus position change for (a) Apuseeq Anittangasikkaajuk (glacier ID 137), where SERMeQ underestimates the true rate of retreat; (b) Helheim Glacier (glacier ID 175), where SERMeQ overestimates retreat; (c) Sermeq Kujalleq (glacier ID 3), where SERMeQ captures observed retreat. Black curves indicate SERMeQ-simulated terminus positions, while blue markers indicate MEaSUREs observations. The blue lines show the most-advanced and most-retreated parts of the terminus projected onto the centerline, and blue diamonds indicate the centroid of the observed terminus projected onto the centerline. Lower left corner annotations give Spearman's rank correlation coefficient ρ between observed and simulated terminus position change for each glacier. Plots share both x- and y-axis scales.
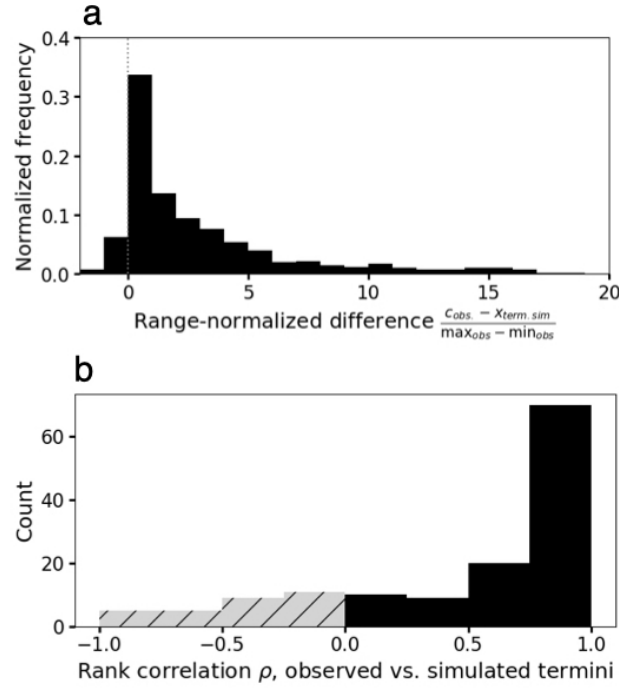
Figure 4. Histograms of (a) Range-normalized difference in terminus position, where the simulated terminus position $x_{\text{term.sim.}}$ is compared with the centroid of the observed terminus c_{obs} and normalized by the range of observed terminus positions ($\max_{\text{obs}}$ - $\min_{\text{obs}}$) along the flowline in the same year; and (b) Spearman's rank-correlation coefficient, ρ, between observed and simulated terminus positions for all glaciers.

3.2 Upper bound retreat rates are realistic

A useful upper bound on calving retreat would consistently overestimate the rate of retreat (Figure 2), simulate terminus positions relatively close to observed termini, and correlate with observed changes. We quantify SERMeQ's performance on the latter indicators in Figure 4.

The histogram in Figure 4a summarizes 404 comparisons of simulated versus observed terminus positions, normalized by each glacier's observational range for each year, such that values within ± 1 indicate simulated terminus positions within the observed range. 40% of simulated terminus positions fall within that range, and 55% of simulated terminus positions are within twice the range of the observed—that is, the simulations are relatively close to the observations. Most simulated terminus positions are more retreated than the observed (positive x-axis values in Figure 4), as expected for an upper bound.

Because we present an upper bound on retreat rather than a calibrated model fit, we do not expect a linear relationship between simulated and observed retreat. Instead, we assess Spearman's rank correlation coefficient for each glacier's terminus positions over time. The coefficient ρ ranges from -1 to 1, where positive ρ indicates that retreat is observed when the model simulates retreat, advance is observed when the model simulates advance, and larger magnitudes of observed and simulated change correspond. Of the 155 glaciers we simulate, ρ is positive for 103, as shown in Figure 4b. For 62 glaciers simulated, $\rho \geq 0.5$ and significant at the $p < 0.1$ level, which indicates a moderately strong and statistically significant relationship between simulated and observed terminus position over time. Only 2 glaciers have negative ρ significant at the same level. The mean ρ over all 155 glaciers is 0.5.

4 Discussion

Our simulated upper-bound rate of terminus retreat/advance emerges as a dynamic glacier response to climate forcing and glacier geometry (Equation 1) and does not rely on any tuning to match observations. The two model parameters, yield strength of glacier ice τ_y and ice temperature T, are physical quantities constrained by laboratory and field observations, and neither is optimized against observed retreat rates. The yield strengths we use for most Greenland outlet glaciers simulated here range from 50-250 kPa (Supplementary Text S3), well within the range of 50-500 kPa suggested by previous works (Nimmo, 2004; O'Neel et al., 2005; Cuffey & Paterson, 2010). We use an ice temperature of $-10°C$, which is also within the range expected from simple physical scaling (van der Veen, 2013), observations (Clow et al., 1996), and modeling (Greuell & Konzelmann, 1994). It is possible an improved match to observed retreat rates could be found if we did allow parameters to vary within and between glacier catchments or over time. However, that would sacrifice the physical upper bound in favor of empirical tuning that cannot be independently constrained by laboratory or field observations.

The upper-bound retreat rate computed from Equation 1 can far exceed the observed rate, as shown in Figures 2 and 3b. There are three notable sources of discrepancy between the modelled and observed retreat rates shown in Figures 2-4: (1) quality of available model input data, (2) performance of automated flowline selection algorithm, and (3) presence of floating ice. First, on small outlets that are rarely visited or studied in detail, the bed topography and climate reanalysis data used as input for SERMeQ may be poorly constrained. As a result, the simulated glacier evolves in response to conditions that do not accurately reflect the local environment, and the simulated change in terminus position is more likely to be inaccurate. Second, on small or slow-moving outlets, or where there are gaps in Sentinel-1 velocity data, our method for tracing flowlines (Text S5) is prone to error. As a result, the simulated glacier has unrealistic geometry

and may flow over bedrock features that are not present in a true central flowline of the outlet. Finally, where floating tongues are present, we remove them and simulate the first grounded grid point as the "terminus". This can change the near-terminus stress state, in some cases exposing an unstable wall of thick ice and initiating rapid retreat. Effects (1) and (2) are likely responsible for the underestimated retreat of Apuseeq Anittangasikkaajuk; effect (3) is likely responsible for the overestimated retreat of Helheim Glacier (see Supplementary Text S6). The first two effects can be mitigated with improved observational data and manual data processing where possible. The third effect reflects upper-bound retreat dynamics that are currently held in check by floating ice, but which we speculate could be activated if that floating ice were removed.

The 91% satisfaction of the intended upper bound on retreat rate (Figure 2) supports the utility of our model for producing upper bounds on calving retreat and dynamic mass loss. In contrast to existing estimates of 21st-century calving loss, our approach does not impose a uniform calving rate or outlet glacier speedup factor (Pfeffer et al., 2008; Graversen et al., 2011; Goelzer et al., 2013; DeConto & Pollard, 2016; Goelzer et al., 2020, accepted); instead, we calculate a theoretical maximum rate of calving retreat that can vary by glacier (Bassis & Ultee, 2019). The result is a physically consistent bound on terminus position change that correlates with observed changes for most glaciers (Figure 4b). By contrast, simpler bounding methods such as imposing a fixed minimum terminus position would have no relationship ($\rho = 0$) with observed terminus position change. Further, our model can track terminus retreat and mass loss from multiple interacting branches of a glacier tributary network (Ultee & Bassis, 2017; Ultee, 2018), ensuring that potentially important contributions to sea level are not overlooked. Within ice-sheet-scale models, our method could be implemented as a calving criterion at grounded ice-ocean interface cells or used as a module to enhance resolution of outlet glacier networks.

The current version of SERMeQ does not explicitly simulate frontal ablation by submarine melting, which can be a large component of mass loss from both floating tongues and grounded glacier fronts (Rignot et al., 2010; Enderlin & Howat, 2013; Wood et al., 2018). Our derivation of Equation 1, which we emphasise is an upper bound on retreat rate, is consistent with high submarine melt that prevents the glacier terminus from advancing (see Supplementary Text S4 and Ma, 2018; Ma & Bassis, 2019). However, changes in ocean conditions over time can affect glacier terminus dynamics such that the rate of terminus position change becomes closer to or farther from the theoretical maximum. For example, a decrease in submarine melt rate has been implicated in the recent slowing of Sermeq Kujalleq's retreat (Khazendar et al., 2019). Future implementations of our method in larger-scale models may therefore benefit from modifications to account for time-varying submarine melt rates.

5 Conclusions

We have applied a flowline network model of ice dynamics, SERMeQ, to evaluate an upper bound on annual to decadal-scale calving retreat of 155 Greenland outlet glaciers in response to variable climate forcing. Comparison with nearly a decade of terminus position records from MEaSUREs (Joughin et al., 2015, updated 2017a) shows that the model bounds retreat rate for 91% of glaciers examined, and that 55% of simulated terminus positions are within twice the observed range. SERMeQ can also evolve upstream surface elevation with each change in terminus position and compute the resultant loss of ice mass above buoyancy (Supplementary Text S1; Ultee, 2018). The upper bound on retreat rate that we construct with SERMeQ will produce a corresponding high-end estimate of the loss of grounded ice mass, consistent with efforts to find an upper bound on the ice-dynamics contribution to 21st century sea level rise. Our approach is especially promising in constraining the dynamic sea level contribution from smaller outlet glaciers that are difficult to resolve in larger-scale continental ice sheet models.

References

Albrecht, T., & Levermann, A. (2012). Fracture field for large-scale ice dynamics. *Journal of Glaciology*, *58*(207), 165–176. doi: 10.3189/2012JoG11J191

Aschwanden, A., Fahnestock, M. A., & Truffer, M. (2016). Complex Greenland outlet glacier flow captured. *Nature Communications*, *7*, 10524 EP. doi: 10.1038/ncomms10524

Aschwanden, A., Fahnestock, M. A., Truffer, M., Brinkerhoff, D. J., Hock, R., Khroulev, C., ... Khan, S. A. (2019). Contribution of the Greenland Ice Sheet to sea level over the next millennium. *Science Advances*, *5*(6). doi: 10.1126/sciadv.aav9396

Bassis, J. N., & Ultee, L. (2019). A thin film viscoplastic theory for calving glaciers: Towards a bound on the calving rate of glaciers. *Journal of Geophysical Research: Earth Surface*, *124*. doi: 10.1029/2019JF005160

Bassis, J. N., & Walker, C. C. (2012). Upper and lower limits on the stability of calving glaciers from the yield strength envelope of ice. *Proceedings of the Royal Society of London A: Mathematical, Physical and Engineering Sciences*, *468*(2140), 913–931. doi: 10.1098/rspa.2011.0422

Beckmann, J., Perrette, M., & Ganopolski, A. (2018). Simple models for the simulation of submarine melt for a Greenland glacial system model. *The Cryosphere*, *12*(1), 301–323. doi: 10.5194/tc-12-301-2018

Benn, D. I., Åström, J., Zwinger, T., Todd, J., Nick, F. M., Cook, S., ... Luckman, A. (2017). Melt-under-cutting and buoyancy-driven calving from tidewater glaciers: new insights from discrete element and continuum model simulations. *Journal of Glaciology*, *63*(240), 691-702. doi: 10.1017/jog.2017.41

Benn, D. I., Cowton, T., Todd, J., & Luckman, A. (2017). Glacier calving in Greenland. *Current Climate Change Reports*, *3*(4), 282–290. doi: 10.1007/s40641-017-0070-1

Borstad, C. P., Khazendar, A., Larour, E., Morlighem, M., Rignot, E., Schodlok, M. P., & Seroussi, H. (2012). A damage mechanics assessment of the Larsen B ice shelf prior to collapse: Toward a physically-based calving law. *Geophysical Research Letters*, *39*(18), L18502. doi: 10.1029/2012GL053317

Brown, C. S., Meier, M. F., & Post, A. (1982). *Calving speed of Alaska tidewater glaciers, with application to Columbia Glacier* (Tech. Rep. No. Geological Survey Professional Paper 1258-C). US Government Printing Office.

Catania, G. A., Stearns, L. A., Sutherland, D. A., Fried, M. J., Bartholomaus, T. C., Morlighem, M., ... Nash, J. (2018). Geometric controls on tidewater glacier retreat in central western Greenland. *Journal of Geophysical Research: Earth Surface*, *123*(8), 2024-2038. doi: 10.1029/2017JF004499

Choi, Y., Morlighem, M., Rignot, E., Mouginot, J., & Wood, M. (2017, 2019/12/18). Modeling the response of Nioghalvfjerdsfjorden and Zachariae Isstrøm glaciers,

Greenland, to ocean forcing over the next century. *Geophysical Research Letters*, *44*(21), 11,071–11,079. doi: 10.1002/2017GL075174

Clow, G. D., Saltus, R. W., & Waddington, E. D. (1996). A new high-precision borehole-temperature logging system used at GISP2, Greenland, and Taylor Dome, Antarctica. *Journal of Glaciology*, *42*(142), 576-584. doi: 10.3189/S0022143000003555

Cuffey, K., & Paterson, W. (2010). *The physics of glaciers* (4th ed.). Elsevier Science, Burlington, MA and Kidlington, United Kingdom. Retrieved from `https://books.google.com/books?id=Jca2v1u1EKEC`

DeConto, R. M., & Pollard, D. (2016). Contribution of Antarctica to past and future sea-level rise. *Nature*, *531*, 591 EP. doi: 10.1038/nature17145

Duddu, R., Bassis, J. N., & Waisman, H. (2013). A numerical investigation of surface crevasse propagation in glaciers using nonlocal continuum damage mechanics. *Geophysical Research Letters*, *40*(12), 3064–3068. doi: 10.1002/grl.50602

Emetc, V., Tregoning, P., Morlighem, M., Borstad, C., & Sambridge, M. (2018). A statistical fracture model for Antarctic ice shelves and glaciers. *The Cryosphere*, *12*(10), 3187–3213. doi: 10.5194/tc-12-3187-2018

Enderlin, E. M., & Howat, I. M. (2013). Submarine melt rate estimates for floating termini of Greenland outlet glaciers (2000–2010). *Journal of Glaciology*, *59*(213), 67–75. doi: 10.3189/2013JoG12J04967

Enderlin, E. M., Howat, I. M., Jeong, S., Noh, M.-J., van Angelen, J. H., & van den Broeke, M. R. (2014). An improved mass budget for the Greenland ice sheet. *Geophysical Research Letters*, *41*(3), 866–872. doi: 10.1002/2013GL059010

Enderlin, E. M., O'Neel, S., Bartholomaus, T. C., & Joughin, I. (2018). Evolving environmental and geometric controls on Columbia Glacier's continued retreat. *Journal of Geophysical Research: Earth Surface*, *123*, 1528 - 1545. doi: 10.1029/2017JF004541

ENVEO. (2017). *Greenland ice velocity map 2016/2017 from Sentinel-1 [version 1.0]*. `http://products.esa-icesheets-cci.org/products/details/greenland_ice_velocity_map_winter_2016_2017_v1_0.zip/`.

Felikson, D., Bartholomaus, T. C., Catania, G. A., Korsgaard, N. J., Kjær, K. H., Morlighem, M., ... Nash, J. D. (2017). Inland thinning on the Greenland ice sheet controlled by outlet glacier geometry. *Nature Geoscience*, *10*(5), 366–369. doi: 10.1038/ngeo2934

Goelzer, H., Huybrechts, P., Fürst, J. J., Nick, F. M., Andersen, M. L., Edwards, T. L., ... Shannon, S. (2013). Sensitivity of Greenland Ice Sheet projections to model formulations. *Journal of Glaciology*, *59*(216), 733-749. doi: 10.3189/2013JoG12J182

Goelzer, H., Nowicki, S., Payne, A., Larour, E., Seroussi, H., Lipscomb, W. H., ... van den Broeke, M. (2020, accepted). The future sea-level contribution of the greenland ice sheet: a multi-model ensemble study of ismip6. *The Cryosphere Discussions*, 1–43. doi: 10.5194/tc-2019-319

Graversen, R. G., Drijfhout, S., Hazeleger, W., van de Wal, R., Bintanja, R., & Helsen, M. (2011). Greenland's contribution to global sea-level rise by the end of the 21st century. *Climate Dynamics*, *37*(7), 1427–1442. doi: 10.1007/s00382-010-0918-8

Greuell, W., & Konzelmann, T. (1994). Numerical modelling of the energy balance and the englacial temperature of the Greenland Ice Sheet. Calculations for the ETH-Camp location (West Greenland, 1155 m a.s.l.). *Global and Planetary Change*, *9*(1), 91–114. doi: 10.1016/0921-8181(94)90010-8

Greve, R. (2000). On the response of the Greenland Ice Sheet to greenhouse climate change. *Climatic Change*, *46*(3), 289–303. doi: 10.1023/A:1005647226590

Hanson, B., & Hooke, R. L. (2000). Glacier calving: a numerical model of forces in the calving-speed/water-depth relation. *Journal of Glaciology*, *46*(153), 188-

196. doi: 10.3189/172756500781832792

Joughin, I., Smith, B., Howat, I. M., & Scambos, T. (2015, updated 2017a). *MEa-SUREs Annual Greenland Outlet Glacier Terminus Positions from SAR Mosaics, Version 1.* NASA National Snow and Ice Data Center Distributed Active Archive Center. Boulder, Colorado USA. doi: https://doi.org/10.5067/DC0MLBOCL3EL

Joughin, I., Smith, B., Howat, I. M., & Scambos, T. (2015, updated 2017b). *MEaSUREs Greenland Ice Sheet Velocity Map from InSAR Data, Version 2.* NASA National Snow and Ice Data Center Distributed Active Archive Center. Boulder, Colorado USA. doi: https://doi.org/10.5067/OC7B04ZM9G6Q

Joughin, I., Smith, B., Howat, I. M., Scambos, T., & Moon, T. (2010). Greenland flow variability from ice-sheet-wide velocity mapping. *Journal of Glaciology*, *56*(197), 415-430. doi: 10.3189/002214310792447734

Khan, S. A., Kjær, K. H., Bevis, M., Bamber, J. L., Wahr, J., Kjeldsen, K. K., . . . Muresan, I. S. (2014). Sustained mass loss of the northeast Greenland ice sheet triggered by regional warming. *Nature Climate Change*, *4*, 292 EP. doi: 10.1038/nclimate2161

Khazendar, A., Fenty, I. G., Carroll, D., Gardner, A., Lee, C. M., Fukumori, I., . . . Willis, J. (2019). Interruption of two decades of Jakobshavn Isbrae acceleration and thinning as regional ocean cools. *Nature Geoscience*, *12*(4), 277–283. doi: 10.1038/s41561-019-0329-3

Krug, J., Weiss, J., Gagliardini, O., & Durand, G. (2014). Combining damage and fracture mechanics to model calving. *The Cryosphere*, *8*(6), 2101–2117. doi: 10.5194/tc-8-2101-2014

Levermann, A., Albrecht, T., Winkelmann, R., Martin, M. A., Haseloff, M., & Joughin, I. (2012). Kinematic first-order calving law implies potential for abrupt ice-shelf retreat. *The Cryosphere*, *6*(2), 273–286. doi: 10.5194/tc-6-273-2012

Lucas-Picher, P., Wulff-Nielsen, M., Christensen, J. H., Aalgeirsdóttir, G., Mottram, R., & Simonsen, S. B. (2012). Very high resolution regional climate model simulations over Greenland: Identifying added value. *Journal of Geophysical Research: Atmospheres*, *117*(D2). doi: 10.1029/2011JD016267

Ma, Y. (2018). *Calving behavior of tidewater glaciers* (Doctoral dissertation, University of Michigan). Retrieved from https://deepblue.lib.umich.edu/handle/2027.42/146058

Ma, Y., & Bassis, J. N. (2019). The effect of submarine melting on calving from marine terminating glaciers. *Journal of Geophysical Research: Earth Surface*, *124*(2), 334–346. doi: 10.1029/2018JF004820

Maussion, F., Butenko, A., Champollion, N., Dusch, M., Eis, J., Fourteau, K., . . . Marzeion, B. (2019). The open global glacier model (OGGM) v1.1. *Geoscientific Model Development*, *12*(3), 909–931. doi: 10.5194/gmd-12-909-2019

Meier, M. F., & Post, A. (1987). Fast tidewater glaciers. *Journal of Geophysical Research: Solid Earth*, *92*(B9), 9051–9058. Retrieved from http://dx.doi.org/10.1029/JB092iB09p09051 doi: 10.1029/JB092iB09p09051

Mercenier, R., Lüthi, M. P., & Vieli, A. (2019). A transient coupled ice flow-damage model to simulate iceberg calving from tidewater outlet glaciers. *Journal of Advances in Modeling Earth Systems*. doi: 10.1029/2018MS001567

Morlighem, M., Bondzio, J., Seroussi, H., Rignot, E., Larour, E., Humbert, A., & Rebuffi, S. (2016). Modeling of Store Gletscher's calving dynamics, West Greenland, in response to ocean thermal forcing. *Geophysical Research Letters*, *43*(6), 2659–2666. doi: 10.1002/2016GL067695

Morlighem, M., Williams, C. N., Rignot, E., An, L., Arndt, J. E., Bamber, J. L., . . . Zinglersen, K. B. (2017). BedMachine v3: Complete bed topography and ocean bathymetry mapping of Greenland from multibeam echo sounding combined with mass conservation. *Geophysical Research Letters*, *44*(21), 11,051-11,061.

doi: 10.1002/2017GL074954

Morlighem, M., Wood, M., Seroussi, H., Choi, Y., & Rignot, E. (2019). Modeling the response of northwest Greenland to enhanced ocean thermal forcing and subglacial discharge. *The Cryosphere*, *13*(2), 723–734. doi: 10.5194/tc-13-723-2019

Mottram, R., Boberg, F., & Langen, P. (2018). *Greenland surface mass balance from Regional Climate Model HIRHAM5.* http://prudence.dmi.dk/data/temp/RUM/HIRHAM/GREENLAND/. Danish Meteorological Institute, Copenhagen, DK.

Mottram, R., Nielsen, K. P., Gleeson, E., & Yang, X. (2017). Modelling glaciers in the HARMONIE-AROME NWP model. *Advances in Science and Research*, *14*, 323–334. doi: 10.5194/asr-14-323-2017

Nick, F. M., Vieli, A., Andersen, M. L., Joughin, I., Payne, A., Edwards, T. L., . . . van de Wal, R. S. W. (2013). Future sea-level rise from Greenland's main outlet glaciers in a warming climate. *Nature*, *497*(7448), 235–238. doi: 10.1038/nature12068

Nimmo, F. (2004). What is the Young's modulus of ice? In *Europa's icy shell.*

Noël, B., van de Berg, W. J., van Wessem, J. M., van Meijgaard, E., van As, D., Lenaerts, J. T. M., . . . van den Broeke, M. R. (2018). Modelling the climate and surface mass balance of polar ice sheets using RACMO2 – Part 1: Greenland (1958–2016). *The Cryosphere*, *12*(3), 811–831. doi: 10.5194/tc-12-811-2018

Nye, J. F. (1951). The flow of glaciers and ice-sheets as a problem in plasticity. *Proceedings of the Royal Society of London A: Mathematical, Physical and Engineering Sciences*, *207*(1091), 554–572. doi: 10.1098/rspa.1951.0140

O'Neel, S., Pfeffer, W. T., Krimmel, R., & Meier, M. (2005). Evolving force balance at Columbia Glacier, Alaska, during its rapid retreat. *Journal of Geophysical Research: Earth Surface*, *110*(F3), F03012. doi: 10.1029/2005JF000292

Pfeffer, W. T., Harper, J. T., & O'Neel, S. (2008). Kinematic constraints on glacier contributions to 21st-century sea-level rise. *Science*, *321*(5894), 1340–1343. doi: 10.1126/science.1159099

Pollard, D., DeConto, R. M., & Alley, R. B. (2015). Potential Antarctic Ice Sheet retreat driven by hydrofracturing and ice cliff failure. *Earth and Planetary Science Letters*, *412*, 112 - 121. doi: 10.1016/j.epsl.2014.12.035

Price, S. F., Lipscomb, W., Hoffman, M., Hagdorn, M., Rutt, I., Payne, T., . . . Kennedy, J. H. (2015). *CISM 2.0.5 Documentation.* `http://oceans11.lanl.gov/trac/CISM/data/cism_documentation_v2.0.pdf`.

Price, S. F., Payne, A. J., Howat, I. M., & Smith, B. E. (2011). Committed sea-level rise for the next century from Greenland ice sheet dynamics during the past decade. *Proceedings of the National Academy of Sciences*, *108*(22), 8978–8983. doi: 10.1073/pnas.1017313108

Rae, J. G. L., Aalgeirsdóttir, G., Edwards, T. L., Fettweis, X., Gregory, J. M., Hewitt, H. T., . . . van den Broeke, M. R. (2012). Greenland ice sheet surface mass balance: evaluating simulations and making projections with regional climate models. *The Cryosphere*, *6*(6), 1275–1294. doi: 10.5194/tc-6-1275-2012

Rignot, E., Koppes, M., & Velicogna, I. (2010). Rapid submarine melting of the calving faces of West Greenland glaciers. *Nature Geoscience*, *3*, 187 EP. doi: 10.1038/ngeo765

Solgaard, A. M., Simonsen, S. B., Grinsted, A., Mottram, R., Karlsson, N. B., Hansen, K., . . . Sørensen, L. S. (2020). Hagen Bræ: A surging glacier in North Greenland—35 years of observations. *Geophysical Research Letters*, *47*(6), e2019GL085802. doi: 10.1029/2019GL085802

Sun, S., Cornford, S. L., Moore, J. C., Gladstone, R., & Zhao, L. (2017). Ice shelf fracture parameterization in an ice sheet model. *The Cryosphere*, *11*(6), 2543–2554. doi: 10.5194/tc-11-2543-2017

Sutherland, D. A., Jackson, R. H., Kienholz, C., Amundson, J. M., Dryer, W. P., Duncan, D., . . . Nash, J. D. (2019). Direct observations of submarine melt and subsurface geometry at a tidewater glacier. *Science*, *365*(6451), 369–374. doi: 10.1126/science.aax3528

Ultee, L. (2018). *Constraints on the dynamic contribution to 21st-century sea level rise from Greenland outlet glaciers* (Doctoral dissertation, University of Michigan). Retrieved from `https://deepblue.lib.umich.edu/handle/2027.42/145794`

Ultee, L., & Bassis, J. N. (2016). The future is Nye: An extension of the perfect plastic approximation to tidewater glaciers. *Journal of Glaciology*, *62*(236), 1143-1152. doi: 10.1017/jog.2016.108

Ultee, L., & Bassis, J. N. (2017). A plastic network approach to model calving glacier advance and retreat. *Frontiers in Earth Science*, *5*(24). doi: 10.3389/feart.2017.00024

van den Broeke, M. R., Box, J., Fettweis, X., Hanna, E., Noël, B., Tedesco, M., . . . van Kampenhout, L. (2017). Greenland Ice Sheet surface mass loss: Recent developments in observation and modeling. *Current Climate Change Reports*, *3*(4), 345–356. doi: 10.1007/s40641-017-0084-8

van den Broeke, M. R., Enderlin, E. M., Howat, I. M., Kuipers Munneke, P., Noël, B. P. Y., van de Berg, W. J., . . . Wouters, B. (2016). On the recent contribution of the Greenland ice sheet to sea level change. *The Cryosphere*, *10*(5), 1933–1946. doi: 10.5194/tc-10-1933-2016

van der Veen, C. (2013). *Fundamentals of glacier dynamics* (2nd ed.). Boca Raton, FL, USA: Taylor & Francis.

Winkelmann, R., Martin, M. A., Haseloff, M., Albrecht, T., Bueler, E., Khroulev, C., & Levermann, A. (2011). The Potsdam Parallel Ice Sheet Model (PISM-PIK) – Part 1: Model description. *The Cryosphere*, *5*(3), 715–726. doi: 10.5194/tc-5-715-2011

Wood, M., Rignot, E., Fenty, I., Menemenlis, D., Millan, R., Morlighem, M., . . . Seroussi, H. (2018). Ocean-induced melt triggers glacier retreat in northwest Greenland. *Geophysical Research Letters*, *45*(16), 8334–8342. doi: 10.1029/2018GL078024